Title

Gas flux and carbonate occurrence at a shallow seep of thermogenic natural gas

Journal

Geo-Marine Letters: An International Journal of Marine Geology, 30(3)

ISSN

1432-1157

Authors

Kinnaman, Franklin S.
Kimball, Justine B.
Busso, Luis
et al.

Publication Date

2010-06-01

DOI

10.1007/s00367-010-0184-0

Peer reviewed

Geo-Mar Lett (2010) 30:355–365
DOI 10.1007/s00367-010-0184-0

ORIGINAL

Gas flux and carbonate occurrence at a shallow seep of thermogenic natural gas

Franklin S. Kinnaman · Justine B. Kimball · Luis Busso · Daniel Birgel · Haibing Ding · Kai-Uwe Hinrichs · David L. Valentine

Received: 22 January 2009 / Accepted: 14 January 2010 / Published online: 20 February 2010

Abstract The Coal Oil Point seep field located offshore Santa Barbara, CA, consists of dozens of named seeps, including a peripheral ~200 m^2 area known as Brian Seep, located in 10 m water depth. A single comprehensive survey of gas flux at Brian Seep yielded a methane release rate of ~450 moles of CH_4 per day, originating from 68 persistent gas vents and 23 intermittent vents, with gas flux among persistent vents displaying a log normal frequency distribution. A subsequent series of 33 repeat surveys conducted over a period of 6 months tracked eight persistent vents, and revealed substantial temporal variability in gas venting, with flux from each individual vent varying by more than a factor of 4. During wintertime surveys sediment was largely absent from the site, and carbonate concretions were exposed at the seafloor. The presence of the carbonates was unexpected, as the thermogenic seep gas contains 6.7% CO_2, which should act to dissolve carbonates. The average $\delta^{13}C$ of the carbonates was −29.2±2.8‰ VPDB, compared to a range of −1.0 to +7.8‰ for CO_2 in the seep gas, indicating that CO_2 from the seep gas is quantitatively not as important as ^{13}C-depleted bicarbonate derived from methane oxidation. Methane, with a $\delta^{13}C$ of approximately −43‰, is oxidized and the resulting inorganic carbon precipitates as high-magnesium calcite and other carbonate minerals. This finding is supported by ^{13}C-depleted biomarkers typically associated with anaerobic methanotrophic archaea and their bacterial syntrophic partners in the carbonates (lipid biomarker $\delta^{13}C$ ranged from −84 to −25‰). The inconsistency in $\delta^{13}C$ between the carbonates and the seeping CO_2 was resolved by discovering pockets of gas trapped near the base of the sediment column with $\delta^{13}C$-CO_2 values ranging from −26.9 to −11.6‰. A mechanism of carbonate formation is proposed in which carbonates form near the sediment–bedrock interface during times of sufficient sediment coverage, in which anaerobic oxidation of methane is favored. Precipitation occurs at a sufficient distance from active venting for the molecular and isotopic composition of seep gas to be masked by the generation of carbonate alkalinity from anaerobic methane oxidation.

Electronic supplementary material The online version of this article (doi:10.1007/s00367-010-0184-0) contains supplementary material, which is available to authorized users.

F. S. Kinnaman · J. B. Kimball · L. Busso · H. Ding · D. L. Valentine (✉)
Department of Earth Science and Marine Science Institute,
University of California,
Santa Barbara, CA 93106, USA
e-mail: valentine@geol.ucsb

D. Birgel · K.-U. Hinrichs
MARUM—Center for Marine Environmental Sciences,
University of Bremen,
P.O. Box 330440, 28334 Bremen, Germany

Present Address:
J. B. Kimball
Department of Environmental Earth System Science,
Stanford University,
Stanford, CA 95064, USA

Introduction

Marine hydrocarbon seeps are seafloor environments with a focused hydrocarbon flux to the overlying waters, and occur along continental margins worldwide (Hovland et al. 1993). Gas seeps are defined by the source and composition of the gas feeding the seep, with biologically generated gas consisting almost entirely of methane, and thermally generated gas often consisting of methane with moderate

levels of carbon dioxide, ethane, propane, and butane. Hydrocarbon seeps have been the subject of intense recent study, particularly on account of their interesting ecology, and their role in the marine methane and carbon cycle (Orphan et al. 2002; Sahling et al. 2002; Boetius and Suess 2004; Levin 2005; Reeburgh 2007). The amount of fossil, radiocarbon-free methane in the atmosphere suggests that natural emission from geological sources (seeps) is significant and possibly underestimated (Etiope et al. 2008). Despite the growing interest in hydrocarbon seep systems, important factors modulating hydrocarbon flux are not well established. For seeps located in deep water and containing dissolved hydrocarbons, important factors include the advective flux of pore fluid through the subsurface (Tryon et al. 2002), the formation of gas hydrate in the subsurface (Suess et al. 1999), and the efficiency of anaerobic, methane-oxidizing communities (Boetius and Suess 2004). Factors known to impact gas seeps in shallow water include the pressure of the underlying gas reservoir (Quigley et al. 1999), blockages or constrictions in fractures and subsequent large "blow-out" events (Leifer et al. 2004), and an imprint of tides on seepage rates (Boles et al. 2001).

The occurrence and formation of carbonate minerals depleted in ^{13}C is common among marine methane seeps (Stakes et al. 1999; Luff and Wallmann 2003; Gieskes et al. 2005; Naehr et al. 2007; Paull et al. 2007), and is used as an indicator of seepage occurrence in the geologic record (Peckmann et al. 1999; Schwartz et al. 2003; Campbell 2006; Gontharet et al. 2007). Carbonate minerals precipitate because of the high carbonate alkalinity associated with vigorous sulfate reduction common to methane seeps. These carbonate minerals are typically depleted in ^{13}C because much of the ambient inorganic carbon is derived from ^{13}C-depleted methane, by way of anaerobic oxidation. Molecular fossils of methane-oxidizing archaea and sulfate-reducing bacteria within ^{13}C-depleted carbonates have a high potential to be preserved (e.g., Peckmann and Thiel 2004). Only recently, molecular fossils of anaerobic methane-oxidizers and their syntrophic partners, sulfate-reducing bacteria, have been described in Late Pennsylvanian seep limestones, showing the syngenicity of molecular fossils and enclosing carbonates (Birgel et al. 2008a). These processes are given in the following equations:

$$CH_4 + SO_4^{2-} \rightarrow HCO_3^- + HS^- + H_2O \quad (1)$$

$$HCO_3^- + Ca^{2+} \rightarrow CaCO_3 + H^+ \quad (2)$$

or

$$2\,HCO_3^- + Ca^{2+} \rightarrow CaCO_3 + CO_2 + H_2O \quad (3)$$

Methane-derived carbonate minerals appear to be rare in seeps with elevated concentrations of CO_2, on account that CO_2 is acidic and tends to cause dissolution of carbonate minerals:

$$CaCO_3 + CO_2 + H_2O \rightarrow 2HCO_3^- + Ca^{2+} \quad (4)$$

For example, methane-derived carbonates have not previously been described in association with the thermogenic gas and oil seeps located near Coal Oil Point, offshore Santa Barbara, CA—arguably the world's most studied.

In this work we describe results from a series of studies conducted at a small seep of thermogenic natural gas located near the Coal Oil Point seep field, offshore Santa Barbara, CA. The magnitude and variability of gas flux are described first, based on measurements made during 80 SCUBA dives to the site. The geochemistry of seep gas and associated carbonate concretions discovered at the site are then described, and finally a hypothesis is developed to better define the conditions enabling formation of these carbonates.

Materials and methods

Study site

The study site for this work was an area of active gas seepage located at 10 m water depth off Campus Point (34° 24.109′N, 119°49.917′W), at the University of California, Santa Barbara (UCSB; Fig. 1a). Known as Brian Seep, this seep encompasses an area of approximately 200 m^2, and spans across two large pipes that transport seawater from farther offshore to the campus. The sediment at Brian Seep is composed primarily of sand, and unlike the sediments in the heart of the nearby Coal Oil Point seeps (Bauer et al. 1988) contains only finely disseminated bits of tar. Previous studies at this site include investigations of aerobic microbial oxidation of natural gas in the sediments (Kinnaman et al. 2007), and methanotrophic microbial mats associated with gas vents (Ding and Valentine 2008).

Gas vent survey

A single comprehensive estimate of the total gas flux for the entirety of Brian Seep was made over the course of ~5 h on 12 September 2004. Seven teams of divers were deployed in succession. Each dive team located a gas vent, quantified the gas flux from the vent, left a numbered marker at the vent, and moved on to the closest unmarked vent. In total, 68 persistent vents were identified and their fluxes quantified. An additional 23 vents were identified,

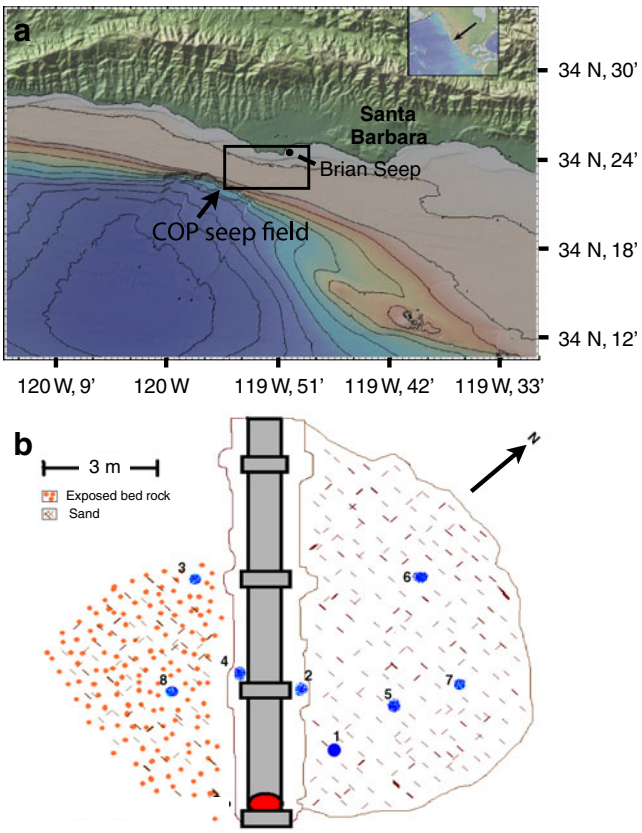

Fig. 1 **a** Area map of the study site. The Coal Oil Point (*COP*) seep field is located within the marked box, with Brian Seep at the northeast periphery as indicated. **b** Relative locations of the eight vents investigated during the time-series flux study. The single pipe illustrated in the diagram represents the two seawater intake pipes described in the text

but with a gas flux too low and inconsistent to quantify. On the final dive, only one persistent vent was identified, and a survey of the entire seep revealed that every active vent was marked. In order to quantify temporal variability of gas flux from Brian Seep, a series of 33 repeat surveys were conducted between 12 July 2005 and 29 November 2005. These surveys focused on quantifying flux from eight persistent vents using the technique described above, but with measurements made in triplicate. The relative spatial distribution for the eight vents is illustrated in Fig. 1b. On several occasions water conditions or safety concerns did not allow for fluxes to be quantified from all active vents.

Gas flux measurements

Gas flux rate was determined by timing the fill rate for a bottle of defined volume (between 70 and 120 cm^3, depending on the apparent voracity of the vent), using an inverted funnel to quantitatively capture the gas in the bottle. Because of safety limitations, only single flux measurements were made for each vent. However, triplicate analyses of individual vents performed in succession on several other occasions yield an error of ±11% for this method. In situ volumes determined by this method were corrected for hydrostatic pressure, temperature, and gas composition to determine the flux of methane. Tide heights ranged from 1.7 to 0.5 m above the mean lower low water for the start and finish of the survey, respectively.

Sediment coverage

During the gas flux surveys, variations were observed in the extent of bedrock exposure at the seafloor. To better quantify the extent of sediment coverage and sediment depth, a series of five repeat surveys were conducted between 26 January 2007 and 3 May 2007. Each survey consisted of three transect lines spaced 10 m apart from each other, with ten measurements per line spaced 1 m apart. The locations of the transects were established to the north of the seawater intake pipes in the vicinity of seeps 2, 5, 6, and 7, and were perpendicular to the pipes. At each station the divers inserted a metal rod into the sediment until bedrock was encountered. The depth of penetration was read from a scale on the metal rod, and the divers then moved to the next station located 1 m further from the intake pipes. The lack of permanent markers for each measurement site likely caused some variations in location between sample dates, and in conjunction with an uncertain bottom topography, impinges on the treatment of the data as a time series.

Sample collection

Samples of gas, sediment, and carbonate were collected from Brian Seep on several occasions during the survey periods. Gas samples were collected from vents as described above for the flux measurements, except that a stopper was inserted in the sample bottle and the bottle was crimp sealed at the seafloor. Carbonate crusts found on the seafloor were collected by SCUBA diver during the wintertime, when sediment burden was low due to offshore sediment transport that is common in the region. Samples were collected throughout the area specified in Fig. 1b, specifically near vents 6, 3, and 8. Samples of the carbonate concretions were removed from the seafloor with a hammer and chisel. A sediment core was collected to quantify depth distributions of dissolved Ca^{2+} in the vicinity of vent 7. Pockets of gas trapped near the base of the sediment column were sampled by probing sediments with a metal rod at 10–20 cm depth, and collecting the displaced gas in a similar manner to seep gas, albeit in smaller (5 mL) glass vials.

Biogeochemical analyses

Gases

Seep gases were analyzed by gas chromatography as previously described by Duffy et al. (2007). Error associated with the concentration measurements was ±4%. All values for $\delta^{13}C$ were referenced to VPDB with an error of ±0.3‰.

Calcium

Calcium analyses were conducted using a Finnigan Element 2 double focusing sector inductively coupled plasma mass spectrometer (ICPMS). The calcium determination was done by measuring the ^{43}Ca isotope and using ^{45}Sc as the internal standard; magnesium determination used a method of isotope dilution by spiking with an enriched ^{25}Mg standard, and measuring ^{24}Mg and ^{25}Mg isotopes (Lea and Martin 1996). Precision of the measurements was based on the Ca and Mg reproducibility of the CS5-B consistency standard. Calcium had a precision estimate of 0.22% rsd and the accuracy was within 1.0% of expected. Magnesium had a precision of 0.33% rsd and the accuracy was within 2.1% of expected.

Carbonates

The mineral composition of the carbonate concretion was estimated by point counting of several thin sections. Point counting was performed on a Zeiss microscope at an interval of 15 µm with an overall count of 600. A polished block of the carbonate was mounted in epoxy and examined using scanning electron microscopy. In the electronic supplementary material available online to authorized users, supplemental Fig. 1 displays an example of a microscope image used in point counting, and an image of carbonates at Brian Seep.

Carbon isotope analysis was performed by dissolving pieces of the concretion in H_3PO_4 (103%, σ=1.92 gml^{-1}), and then analyzing the resulting CO_2 by isotope ratio mass spectrometry (IRMS). Samples were carefully chipped from individual visible layers within the carbonate rock. CO_2 gas was analyzed on a Finnigan Delta XP isotope ratio mass spectrometer coupled with a Finnigan GasBench II at UCSB, within 1 week of preparation. Precision for this measurement was ±0.2‰. Calibration and accuracy of the measurements were assured by running samples of the standards NBS-19 and SM 92 that were prepared in the exact same manner as the carbonate samples. All carbon samples are expressed relative to VPDB.

Lipid biomarkers

Lipids were extracted from subsamples of the carbonate concretion by first dissolving the concretion in HCl (6 M), and extracting the residue after carbonate dissolution. Only inner portions of the rock were used in analysis. Fatty acid extraction and analysis, including quantification, identification, and isotope analysis of individual lipids, were performed on the dissolved carbonate as described in Ding and Valentine (2008). A sample of carbonate was also used to extract polar lipids, neutral lipids, and hydrocarbons for subsequent analysis by GC-IRMS, as described by Birgel et al. (2006, 2008b).

Results

Gas flux

Molecular and isotopic composition of gas samples collected at the seafloor indicated that Brian Seep gas was primarily thermogenic (Table 1), though no oil was emitted at the site. The gas consisted of 91.2% methane and 6.7% CO_2. A subset of data from Table 1 is reposted in this issue by Mau et al. (2010).

Based on the single comprehensive estimate of the total gas flux for the entirety of Brian Seep, and based on a methane content of 91.2%, we estimate a daily methane flux of 435 mol, equivalent to 2.54 tons (t) per year of methane emanating from persistent vents for a 200-m^2 area. The contribution of intermittent vents can also be estimated by assuming a flux equal to half the slowest rate measured during the survey, an assumption supported by diver observations. Based on this assumption, the 23 observed intermittent vents would contribute an additional 0.065 t per year, bringing the total flux for Brian Seep to 2.60 t CH_4 per year (or 448 mol day^{-1}). A frequency distribution of vent seepage intensity is shown in Fig. 2, with an average venting rate of 6.4 mol CH_4 day^{-1} and a maximum observed flux of 30 mol CH_4 day^{-1} for a single vent. The frequency distribution of flux for persistent vents approximately follows a log normal distribution, based on these 68 measurements.

Eight vents were initially chosen for repeat flux measurements in order to better understand the temporal variability associated with gas seeps. Two of these vents (1 and 4) went dormant after a period of ~1 month, and two additional vents were inconsistent (2 and 3) and often found to have no gas flux. Vents with zero flux on a given day were excluded for that day, for all calculations. Summary statistics for each vent, including average flux and the number of times each vent was sampled, are displayed in Table 2. The total number of measurements conducted for

Table 1 $\delta^{13}C$ values of the free gas (collected at the sediment–water column interface), trapped gas (displaced from within sediment), carbonates, and selected biomarker compounds[a]

Compound	$\delta^{13}C$ (‰)	Range	Comment
Free gas			
CH_4	−42.3	−41.9 to −42.6	91.2% of seep gas, n=2
CO_2	3.5	−1.0 to +7.8	6.7% of seep gas, n=2
C_2H_6	−30.0	−27.8 to −32.1	1.0% of seep gas, n=2
C_3H_8	−21.9	−18.3 to −27.1	0.2% of seep gas, n=2
Trapped gas			
CH_4	−41.0±0.8	−40.5 to −42.5	n=5
CO_2	−20.3±7.0	−11.6 to −26.9	n=5
Carbonates			
Concretion 1	−27.8±2.8	−13.2 to −30.9	n=8
Concretion 2	−29.1±1.6	−25.7 to −31.0	n=8
Concretion 3	−29.7±1.5	−26.5 to −33.1	n=31
Select biomarkers			
Archaeol	−84		Methanotrophic archaea
sn-2 OH-Archaeol	−74		Methanotrophic archaea
sn-3 OH-Archaeol	−83		Methanotrophic archaea
PMI	−73		Methanotrophic archaea
Biphytanic diacid (acyclic)	−57		Methanotrophic archaea
Biphytanic diacid (monocyclic)	Trace levels		Methanotrophic archaea
Biphytanic acid (bicyclic)	−80		Methanotrophic archaea
i-$C_{15:0}$	−46		Sulfate-reducing bacteria
a-$C_{15:0}$	−47		Sulfate-reducing bacteria
$C_{16:0}$MAGE	−46		Sulfate-reducing bacteria
$C_{30:0}$DAGE (*ai*-C15/*ai*-C15)	−61		Sulfate-reducing bacteria
bisnor-Hopane	−27		Seep oils
nor-Hopane	−27		Seep oils
Hopane	−27		Seep oils
n-$C_{16:0}$	−28		Broadly sourced
n-$C_{18:0}$	−27		Broadly sourced
Other organics present			
Monterey oil	−22.5	−21.8 to −23.3	Orr (1986)
Regional organic matter	−21.5	−20 to −24	See refs. in text

[a] The full range of biomarkers analyzed is available in supplemental Table 3

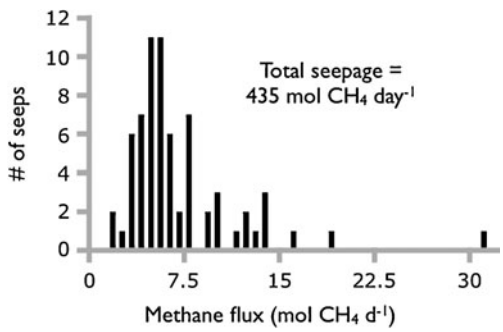

Fig. 2 Histogram displaying the frequency distribution of gas flux for all 68 active vents at Brian Seep measured during the single comprehensive survey. Bin size = 0.75 mol CH_4 day^{-1}. The extrapolated annual flux from these measurements equals 2.5±0.3 t

all eight vents over the 33 sampling trips was 152. Figure 3 displays the full time series for all vents. Figure 3a contains the three most consistently sampled vents (5, 7, and 8), which have overlapping measurements for 21 days. Figure 3b shows the full time series for the other five vents. Similar patterns of flux are apparent for vents 5 and 7 (Fig. 3a), which are closely spaced and relatively vigorous, whereas the weaker vent ~10 m away (seep 8) shows less similarity. The data resolution for the other seeps is insufficient to assess any potential trends. Tidal influences were not apparent. Regressions of gas flux versus tide height for the two most vigorous vents (5 and 7) resulted in a coefficient of determination (R^2) of only 0.15. The time-series data presented in Fig. 3a provided an opportunity to generate an error estimate for the methane flux determined for all of Brian Seep. This was achieved by determining the

Table 2 Average flux rates for the eight vents investigated during the time-series study

Seep	Average (mol CH_4 day^{-1})	±SD	*n*	Min.	Max.
1	5.0	4.1	7	2.4	11.1
2	7.4	3.2	21	3.1	15.8
3	6.0	3.3	14	1.8	14.7
4	7.0	3.1	8	2.5	10.8
5	13.8	4.4	30	2.3	22.9
6	6.0	2.4	22	1.8	11.0
7	21.2	8.2	29	7.8	39.4
8	4.9	1.9	21	2.1	9.9
Σ5, 7, and 8	41.4	10.6	19	18.0	60.5

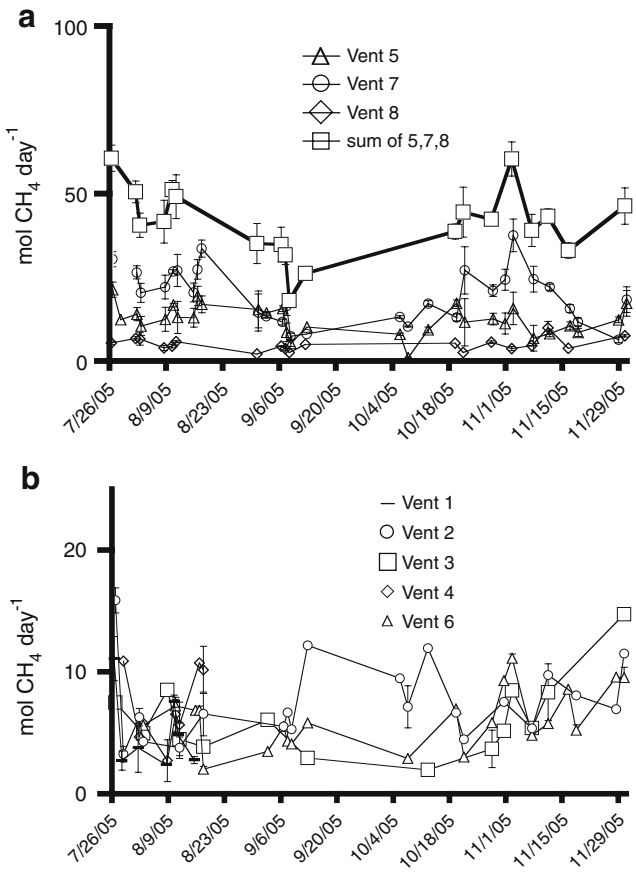

Fig. 3 Results from the time-series flux measurements for eight vents at Brian Seep. **a** Seeps 5, 7, and 8 are displayed together, as they share a large number of common sampling days (21). **b** Seeps 1, 2, 3, 4, and 6 are displayed together, but all share only one common sampling day. Error bars represent one standard deviation from the mean (n=3). Symbols without error bars denote a lack of replicate measurements. The lines are present only for purposes of visual tracking of each seep, and do not imply that flux was continually increasing or decreasing between data points

relative standard deviation of the average flux summed from seeps 5, 7, and 8 (Fig. 3a), for the full time series (n= 21). The error on the flux estimate from Brian Seep is therefore conservatively estimated at ±25%, yielding a flux estimate of 2.7±0.7 t CH_4 $year^{-1}$ for the entire seep.

The variability of gas flux from individual vents can also be analyzed for Brian Seep using the results of the time-series flux study. The frequency distribution for gas flux from all seeps is displayed in Fig. 4a, and suggests a log normal trend for overall flux. The variation in flux for all seeps, with individual seeps normalized to the maximum observed for that seep, is displayed in Fig. 4b, and reveals an approximately normal distribution. Visual observations from this site also revealed potential "blow-out" structures that may arise from periodic release of significantly greater amounts of gas, a phenomenon observed previously in the Coal Oil Point (COP) seep field (Leifer et al. 2004).

Sediment processes

Carbonates

All carbonate samples were a matrix of calcite and aragonite, as well as small crystals of other minerals. Carbonate concretions sampled from the seafloor were

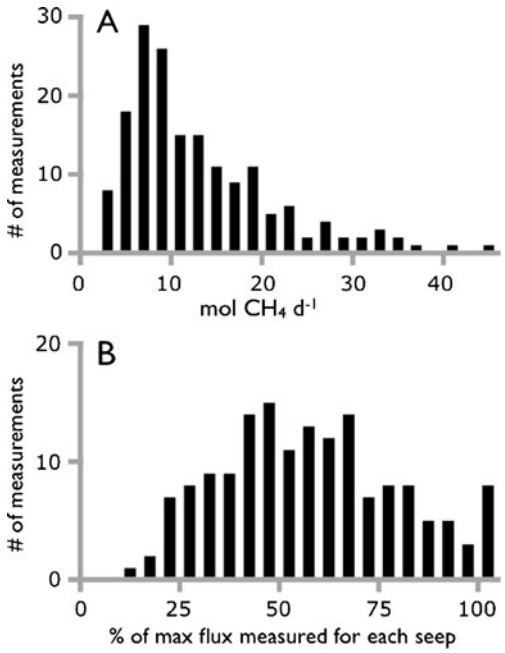

Fig. 4 **a** Histogram displaying the frequency distribution of gas flux including all measurements from all vents during the time-series experiment. Bin size = 2 mol CH_4 day^{-1}. **b** Histogram displaying the frequency distribution for the variation in flux for all vents during the time-series experiment. All flux measurements from each vent were normalized to the maximum observed for that vent, and data from all eight vents aggregated. Bin size = 5% mol CH_4 day^{-1}

found to be consistently depleted in ^{13}C, with an average $\delta^{13}C$ value of −29.2±2.8‰ (values for individual samples are presented in Table 1). ICP-MS analyses found that Ca contents averaged 4.1 mass% of the concretion, and Mg contents 0.83 mass%, a ratio of 5:1. Elemental analyses before and after acidification denote an inorganic carbon content of 1.48 mass%. Although there is likely a minor amount of plagioclase feldspar in the rock that would contribute some Ca and Mg, these results indicate that ~90% is associated with the carbonate cement. Point counting of carbonates established the sampled rocks as quartz-carbonate concretions, with 47.1% of points as quartz mineral, 29.6% calcite cement, 1.5% aragonite, 9.3% pore space, and 12.3% of points found to have small crystals of other minerals. The apparent overrepresentation of calcite cement by point counting is reasonable, as it is likely a matrix of carbonate mixed with small crystals of quartz and other minerals. It is unlikely that much of the carbonate is in the form of dolomite, as it reacted violently with acid. The carbonate cement is most likely a high-magnesium calcite, with some variability in composition throughout the rock. Supplemental Fig. 2 displays an image of a carbonate sample taken with scanning electron microscopy, showing small rosette-shaped crystals of high-Mg calcite growing on a quartz grain.

Sediment coverage

Surveys indicate fluctuations in sediment cover over a 3-month time period in the winter and spring of 2007, with average sediment cover ranging from a low of 11 cm to a high of 22 cm (n=30 at each time point), with rare pockets extending to depths as great as 50 cm. Supplemental Table 1 provides these results. No surveys were conducted in the summer for logistical reasons, but evidence from coring and other investigations at this site indicates a greater sediment burden from late spring through fall, consistent with regional patterns (Patsch and Griggs 2006).

Calcium

One core was collected from the shallow sediments within Brian Seep and used to assess whether Ca^{2+} was being released or precipitated in the sediments, at least for the one site. Relative to overlying seawater, concentrations of Ca^{2+} in the pore fluids were substantially elevated throughout the core, by as much as 38% (supplemental Table 2). Elevated levels of Ca^{2+} are likely due to carbonate dissolution in the presence of carbonic acid, an expected feature of carbonate speciation in porewaters around seeps with a consistent input of gaseous CO_2.

Lipid biomarkers

In order to determine if anaerobic oxidation of methane (AOM) was involved in formation of the carbonates, organic biomarkers were extracted from two separate samples and analyzed for their $\delta^{13}C$. Only fatty acids were analyzed from the first sample, but the presence of fatty acids such as $C_{17:0}$, *iso*-$C_{15:0}$, and *anteiso*-$C_{15:0}$ with $\delta^{13}C$ values ranging from −47 to −39‰ suggests the presence of sulfate-reducing bacteria associated with AOM. The second carbonate underwent a more exhaustive extraction allowing for the separation and identification of other compounds (all data presented in Table 1 and supplemental Table 3). Biomarkers typically associated with seep oils from COP were present in the chromatograms along with a broad unresolved complex mixture, as is typical of the Monterey-derived oils at COP (Orr 1986; Wardlaw et al. 2008; Farwell et al. 2009). Dozens of other compounds were resolved but co-eluted with the unresolved complex mixture (UCM), which likely impacts the accuracy of assigned $\delta^{13}C$ values. Still, archaeal biomarkers of anaerobic methanotrophs such as archaeol, *sn-2* and *sn-3* hydroxyarcheol, and 2, 6, 10, 15, 19-pentamethylicosane (PMI) were identified in the sample with $\delta^{13}C$ values ranging from −84 to −73‰. Further archaeal compounds are biphytanic diacids with 0, 1, and 2 pentacylic rings. The bicyclic biphytanic diacid was found with a $\delta^{13}C$ value of −80‰, whereas the acylic form was found with −57‰. The monocyclic biphytanic diacid was found only in trace amounts.

Gases

The discrepancy in ^{13}C content between seep gas CO_2 (−1.0 to +7.8‰) and the carbonates (−29.3±2.8‰) led us to search for isolated gas pockets that might reveal the biogeochemical conditions allowing these carbonates to form. Probing of sediments with a metal rod released trapped gases from near the base of the sediment with $\delta^{13}C$-CO_2 values ranging from −11.6 to −26.9‰ (summarized in Table 1).

Discussion

Gas flux

Anecdotal evidence has long suggested that gas seeps are highly dynamic environments, but little evidence has been provided to constrain variability in gas flux. Studies on the amount of seep gas captured by two large steel tents open to the seafloor at 80 m depth ~1 km offshore in the COP seep field suggested a long-term influence of offshore oil production (Quigley et al. 1999), and an imprint of tidal

patterns (Boles et al. 2001). These studies demonstrated that the seepage rate varied by a factor of 3 over a 17-year collection period. Evidence from hourly monitoring of the seep tent over a 9-month period by the latter study suggested a variation of only 6% in seepage. A several hour-long study at a shallower seep observed sporadic gas ejection events, and proposed temporary blockages or constrictions in subsurface migration pathways (Leifer et al. 2004). Although Brian Seep is a minor seep constituting only ~0.01% of the total gas flux for the COP seeps, the processes recorded there are likely to occur throughout the seep field. The time-series flux study did not reveal any marked relationship between gas flux and tide or wave height. Short- and long-term variations in flux rate could be responsible for this feature of the dataset. Despite taking triplicate measurements of vent flux when possible, the short sampling time of minutes for each bottle could yield fluxes different from the hour or daylong averages. Long-term changes in gas flux rate are evident in Fig. 3, and could easily overwhelm tidal imprints on flux rate. The observed variability appeared more randomly distributed, suggesting that subsurface plumbing and interplay between active vents may prove a greater cause of variability for the flux of individual vents on weekly to monthly time scales. When viewed collectively, gas flux from all of the vents during the single comprehensive 1-day study (Fig. 2) and the months-long time series (Fig. 4a) was log normal in frequency distribution. Shifting gas flux between select vents could cause this narrow distribution, while individual gas vents display a wider flow range (Fig. 4b). It is possible that flux for individual vents is evenly distributed around an average value based on the subsurface properties of the individual vent, and that net flux is relatively constant. These observations do not constrain previously proposed mechanisms of seep behavior (Tryon et al. 2002; Leifer et al. 2004), or the variability in overall flux from Brian Seep, which could well have remained constant over the entire observation period despite the observed fluctuations in gas flux for specific vents recorded in this study.

Lipid biomarkers

In various ancient seep sites, biphytanic diacids have been described with light $\delta^{13}C$ values and have been suggested as synthetic products of as yet unknown methane-oxidizing archaea (Birgel et al. 2008b). In addition, signals of sulfate-reducing bacteria were identified, such as *iso*-$C_{15:0}$ and *anteiso*-$C_{15:0}$ (−46 and −47‰, respectively). The presence of abundant C_{30}-dialkylglycerolether (DAGE) with two *anteiso*-$C_{15:0}$ alkyl chains and a $\delta^{13}C$ value as low as −61‰ further confirms the presence of sulfate-reducing bacteria (see also Hinrichs et al. 2000; Pancost et al. 2001). Although these biomarkers are not as depleted as at other seep sites (Elvert et al. 2005), most likely due to the ^{13}C-enriched thermogenic methane source, these results indicate that AOM was a prevalent process in the sediment that gave rise to the carbonate concretion.

Subsurface gas pockets

The more ^{13}C depleted of the CO_2 samples from the subsurface gas pockets (listed as "trapped gas" in Table 1) are similar in isotopic composition to the carbonates, and this observation provides insight into how the appropriate conditions are created to enable carbonate formation in these thermogenic gas seeps. Importantly, the five gas samples collected came from between gas vents, away from the immediate impact of gas seepage.

Carbonates

Methane-derived carbonate minerals have not been previously observed in the COP seep field. The carbonates are more depleted than several potential source materials including seawater (−0.3‰ at Brian Seep; Ding and Valentine 2008), seep gas CO_2 (−1.0 to +7.8‰; Table 1), regional organic matter (approx. −20 to −24‰; Silverberg et al. 2004; Ramirez-Alvarez et al. 2007; Li et al. 2009), and local seep oils (−23.4 to −22.7‰; Wardlaw et al. 2008), which strongly suggests that methane was a significant source of carbon, and that anaerobic oxidation of methane (AOM) was important. Subsequent investigations focused on the composition of the carbonates and the biogeochemistry facilitating their formation. Their presence at the base of the sediment column at Brian Seep was unexpected because of the high concentration of isotopically enriched CO_2 present in the seep gas. Based on their composition and pattern of occurrence, we have formulated a hypothesis as to how they form and persist at Brian Seep, a schematic for which is given in Fig. 5. As with other seep environments, carbonate formation is linked with AOM in the shallow subsurface (Stakes et al. 1999; Michaelis et al. 2002; Luff and Wallmann 2003; Formolo et al. 2004; Sassen et al. 2004; Reitner et al. 2005), but several processes distinguish carbonate formation at Brian Seep.

First, carbonate alkalinity must overcome the elevated P_{CO2} associated with the seep gas, which reaches ~15 kPa at Brian Seep. This is presumably accomplished by vigorous sulfate reduction coupled to AOM, though the flux of CO_2 is likely far greater than the capacity of the microbial community to oxidize methane. Spatial segregation of seeping CO_2 and methane is also therefore likely to play an important role. Because CO_2 dissolves rapidly in alkaline solutions, the lateral migration of vent gas near the base of the sediment column may act to "scrub" CO_2 from the gas. At some distance from the main vent, the P_{CO2} may be sufficiently low

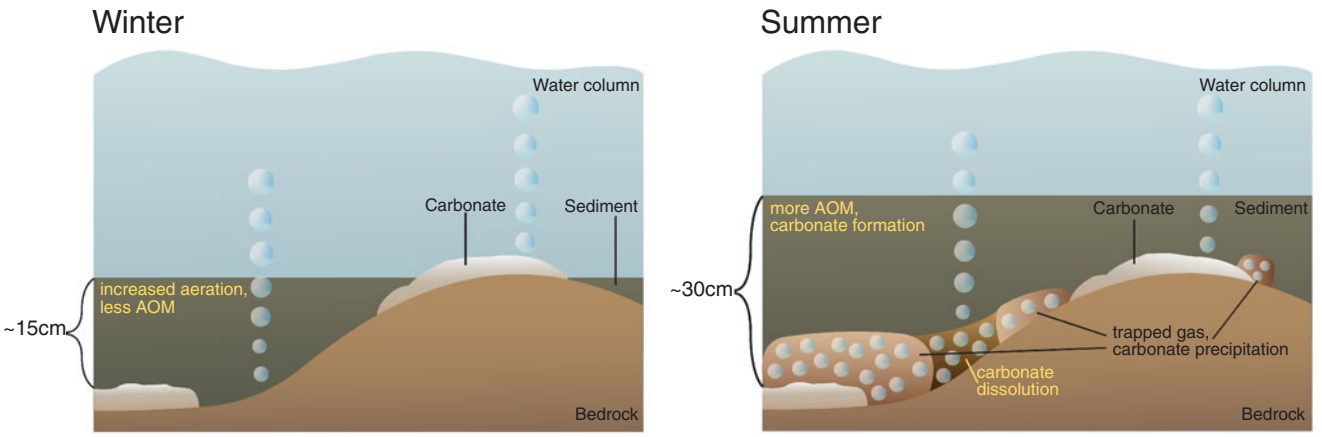

Fig. 5 Schematic diagram highlighting the processes modulating carbonate formation at Brian Seep during times of high and low sediment burden

that, combined with active AOM, sufficient alkalinity could be generated to enable carbonate precipitation.

Second, sufficient methane must be oxidized anaerobically to draw the $\delta^{13}C$ of dissolved inorganic carbon (DIC) from as much as +8‰ in the seep gas to −30‰ in the trapped gas (Table 1). While a simple mass balance calculation would suggest that more than half of the carbonate carbon is derived from methane with a $\delta^{13}C$ of −42‰, the actual proportion may be somewhat lower on account of undetermined contributions from sediment organic matter, other trace seep gases or seawater DIC, and because of carbon isotope fractionation during AOM.

Third, the discovery of distinct $\delta^{13}C$-CO_2 in trapped gases was fortuitous, and suggests that trapping of gas near the base of the sediment column may provide an important mechanism to supply sufficient methane to drive AOM. The locations of trapped gas were on the order of a meter or more from any individual vent, suggesting that lateral migration or a discontinuous underlying source supplied the gas. The slight enrichment in $\delta^{13}C$-CH_4 and depletion in $\delta^{13}C$-CO_2 suggest that these gases may be trapped for extended periods of time, and serve as reservoirs of methane to microbial communities performing AOM. Anaerobic oxidation of methane typically leads to an enrichment in $\delta^{13}C$ of CH_4 and a depletion in $\delta^{13}C$ of CO_2 (Alperin et al. 1988). The observation of enriched $\delta^{13}C$-CH_4 and depleted $\delta^{13}C$-CO_2 in the trapped gas strongly suggests that these bubbles serve as a reservoir, and equilibrate with dissolved CH_4 and DIC. Also, CO_2 was present only at trace levels in the trapped gas, further consistent with the high alkalinities typical of environments harboring AOM. While the data presented here are insufficient to distinguish the location where CO_2 is removed along the migratory pathway, the elevated concentrations of Ca^{2+} in pore fluids from one core suggest that in some areas of the seep field net dissolution of carbonate is likely, presumably related to P_{CO2} as high as 15 kPa. The carbonate-rich areas of the seep field are obviously not dominated by dissolution, however, suggesting strong P_{CO2} gradients near active gas vents.

Fourth, the seasonal loss of sediment from Brian Seep likely alters the biogeochemical conditions that enable carbonate formation. AOM seemingly requires strictly anoxic conditions (Valentine and Reeburgh 2000), but also requires fluxes of both methane and sulfate, typically limiting this process to the shallow marine subsurface where these conditions occur. Therefore, we sought to constrain the extent of sediment habitable to anaerobic methanotrophs at Brian Seep by quantifying sediment burden. In areas of complete sediment removal, AOM may shift into the harder rocks and gravel below the sediments. However, we predict that AOM facilitates carbonate formation primarily when sediment is present in summer and fall after sufficient time has elapsed for slow-growing methanotrophic communities to reestablish themselves after being physically removed in the wintertime, and a build-up of alkalinity in the interstitial porewater occurs. This scenario is supported by the presence of multiple and clearly distinct layers in the carbonate concretion (supplemental Fig. 3). These layers likely represent changing environmental conditions that favor carbonate precipitation, and could well be seasonal.

Lastly, the carbonate concretions formed at Brian Seep consist primarily of quartz sand held together by calcite. These concretions appear to form at the interface of the sediment and underlying bedrock, and thus take on the appearance of exposed bedrock. This mode of occurrence is distinct from methane-derived carbonates from other seep environments (Bohrmann et al. 1998; Michaelis et al. 2002; Gieskes et al. 2005; Niemann et al. 2006), where sulfate penetration and AOM are limited to the upper sediment column. The occurrence of quartz sand cemented by ^{13}C-

depleted carbonates may serve as a distinguishing feature of shallow water gas seeps in the appropriate geologic context.

Conclusions

This study demonstrates the dynamic nature of a shallow seep environment in which gas flux from vents consistently varies, and where seasonal changes directly impact the biogeochemistry of the shallow subsurface. Inundation by sediment seemingly facilitates the precipitation of carbonate minerals at the base of the sediment column, despite the presence of elevated CO_2 concentrations in seep gas. Trapped pockets of free gas are suggested as important reservoirs feeding AOM. Removal of sediments exposes methane-derived carbonates, and presumably removes the communities mediating the anaerobic oxidation of methane. These factors appear to modulate carbonate formation and dissolution in the vicinity of Brian Seep. These observations provide a useful baseline for the behavior of shallow gas seeps in terms of their flux variability, biogeochemistry, and the associated mineralogy.

Acknowledgements We acknowledge Dave Farrar, Shane Anderson, and Georges Paradis for technical support. This research was funded by the United States National Science Foundation (OCE 0447395 to D.L.V.), the University of California Undergraduate Research and Creative Activities Program (to J.K.), and the UC LEADS program (to L.B.). Biomarker analysis at the Univ. of Bremen were supported by the Deutsche Forschungsgemeinschaft through MARUM Research Area "Seepage of Fluid and Gas".

References

Alperin MJ, Reeburgh WS, Whiticar MJ (1988) Carbon and hydrogen isotope fractionation resulting from anaerobic methane oxidation. Global Biogeochem Cycles 2:279–288

Bauer JE, Montagna PA, Spies RB, Prieto MC, Hardin D (1988) Microbial biogeochemistry and heterotrophy in sediments of a marine hydrocarbon seep. Limnol Oceanogr 33:1493–1513

Birgel D, Thiel V, Hinrichs KU, Elvert M, Campbell KA, Reitner J, Farmer JD, Peckmann J (2006) Lipid biomarker patterns of methane-seep microbialites from the Mesozoic convergent margin of California. Org Geochem 37:1289–1302

Birgel D, Himmler T, Freiwald A, Peckmann J (2008a) A new constraint on the antiquity of anaerobic oxidation of methane: late Pennsylvanian seep limestones from southern Namibia. Geology 36:543–546

Birgel D, Elvert M, Han XQ, Peckmann J (2008b) C-13-depleted biphytanic diacids as tracers of past anaerobic oxidation of methane. Org Geochem 39:152–156

Boetius A, Suess E (2004) Hydrate Ridge: a natural laboratory for the study of microbial life fueled by methane from near-surface gas hydrates. Chem Geol 205:291–310

Bohrmann G, Greinert J, Suess E, Torres M (1998) Authigenic carbonates from the Cascadia subduction zone and their relation to gas hydrate stability. Geology 26:647–650

Boles JR, Clark JF, Leifer I, Washburn L (2001) Temporal variation in natural methane seep rate due to tides, Coal Oil Point area, California. J Geophys Res-Oceans 106:27077–27086

Campbell KA (2006) Hydrocarbon seep and hydrothermal vent paleoenvironments and paleontology: past developments and future research directions. Palaeogeogr Palaeoclimatol Palaeoecol 232:362–407

Ding H, Valentine DL (2008) Methanotrophic bacteria occupy benthic microbial mats in shallow marine hydrocarbon seeps, Coal Oil Point, California. J Geophys Res-Biogeosci 113:G01015. doi:10.1029/2007JG000537

Duffy M, Kinnaman F, Valentine DL, Keller E, Clark JF (2007) Gaseous emission rates from natural petroleum seeps in the Upper Ojai Valley, California. Environ Geosci 14:197–207

Elvert M, Hopmans EC, Treude T, Boetius A, Suess E (2005) Spatial variations of methanotrophic consortia at cold methane seeps: implications from a high-resolution molecular and isotopic approach. Geobiology 3:195–209

Etiope G, Lassey KR, Klusman RW, Boschi E (2008) Reappraisal of the fossil methane budget and related emission from geologic sources. Geophys Res Lett 35:L09307. doi:10.1029/2008GL033623

Farwell C, Reddy CM, Peacock E, Nelson RK, Washburn L, Valentine DL (2009) Weathering and the fallout plume of heavy oil from strong petroleum seeps near Coal Oil Point, CA. Environ Sci Technol 43:3542–3548

Formolo MJ, Lyons TW, Zhang CL, Kelley C, Sassen R, Horita J, Cole DR (2004) Quantifying carbon sources in the formation of authigenic carbonates at gas hydrate sites in the Gulf of Mexico. Chem Geol 205:253–264

Gieskes J, Mahn C, Day S, Martin JB, Greinert J, Rathburn T, McAdoo B (2005) A study of the chemistry of pore fluids and authigenic carbonates in methane seep environments: Kodiak Trench, Hydrate Ridge, Monterey Bay, and Eel River Basin. Chem Geol 220:329–345

Gontharet S, Pierre C, Blanc-Valleron MM, Rouchy JM, Fouquet Y, Bayon G, Foucher JP, Woodside J, Mascle J (2007) Nature and origin of diagenetic carbonate crusts and concretions from mud volcanoes and pockmarks of the Nile deep-sea fan (eastern Mediterranean Sea). Deep-Sea Res II-Topical Stud Oceanogr 54:1292–1311

Hinrichs KU, Summons RE, Orphan VJ, Sylva SP, Hayes JM (2000) Molecular and isotopic analysis of anaerobic methane-oxidizing communities in marine sediments. Org Geochem 31:1685–1701

Hovland M, Judd AG, Burke RA (1993) The global flux of methane from shallow submarine sediments. Chemosphere 26:559–578

Kinnaman FS, Valentine DL, Tyler SC (2007) Carbon and hydrogen isotope fractionation associated with the aerobic microbial oxidation of methane, ethane, propane and butane. Geochim Cosmochim Acta 71:271–283

Lea DW, Martin PA (1996) A rapid mass spectrometric method for the simultaneous analysis of barium, cadmium, and strontium in foraminifera shells. Geochim Cosmochim Acta 60:3143–3149

Leifer I, Boles JR, Luyendyk BP, Clark JF (2004) Transient discharges from marine hydrocarbon seeps: spatial and temporal variability. Environ Geol 46:1038–1052

Levin LA (2005) Ecology of cold seep sediments: interactions of fauna with flow, chemistry and microbes. Oceanogr Mar Biol Annu Rev 43:1–46

Li C, Sessions A, Kinnaman F, Valentine DL (2009) Hydrogen-isotopic variability in lipids from Santa Barbara Basin sediments. Geochim Cosmochim Acta 73:4803–4823

Luff R, Wallmann K (2003) Fluid flow, methane fluxes, carbonate precipitation and biogeochemical turnover in gas hydrate-bearing sediments at Hydrate Ridge, Cascadia Margin: numerical modeling and mass balances. Geochim Cosmochim Acta 67:3403–3421

Mau S, Heintz MB, Kinnaman FS, Valentine DL (2010) Compositional variability and air–sea flux of ethane and propane in the plume of a large, marine seep field near Coal Oil Point, CA. In: Bohrmann G, Jørgensen BB (eds) Proc 9th Int Conf Gas in Marine Sediments, 15–19 September 2008, Bremen. Geo-Mar Lett SI 30

Michaelis W, Seifert R, Nauhaus K, Treude T, Thiel V, Blumenberg M, Knittel K, Gieseke A, Peterknecht K, Pape T, Boetius A, Amann R, Jorgensen BB, Widdel F, Peckmann JR, Pimenov NV, Gulin MB (2002) Microbial reefs in the Black Sea fueled by anaerobic oxidation of methane. Science 297:1013–1015

Naehr T, Eichhubl P, Orphan VJ, Hovland M, Paull C, Ussler W, Lorenson TD, Greene G (2007) Authigenic carbonate formation at hydrocarbon seeps in continental margin sediments: a comparative study. Deep-Sea Res II-Topical Stud Oceanogr 54:1268–1291

Niemann H, Duarte J, Hensen C, Omoregie E, Magalhaes VH, Elvert M, Pinheiro LM, Kopf A, Boetius A (2006) Microbial methane turnover at mud volcanoes of the Gulf of Cadiz. Geochim Cosmochim Acta 70:5336–5355

Orphan VJ, House CH, Hinrichs KU, McKeegan KD, DeLong EF (2002) Multiple archaeal groups mediate methane oxidation in anoxic cold seep sediments. Proc Natl Acad Sci USA 99:7663–7668

Orr WL (1986) Kerogen/asphaltene/sulfur relationships in sulfur-rich Monterey oils. Org Geochem 10:499–516

Pancost RD, Bouloubassi I, Aloisi G, Sinninghe Damsté JS, the Medinaut Shipboard Scientific Party (2001) Three series of non-isoprenoidal dialkyl glycerol diethers in cold-seep carbonate crusts. Org Geochem 32:695–707

Patsch K, Griggs G (2006) Littoral cells, sand budgets, and beaches: understanding California's shoreline. In: Institute of Marine Sciences, University of California, Santa Cruz, CA, pp 1–35

Paull CK, Ussler W, Peltzer ET, Brewer PG, Keaten R, Mitts PJ, Nealon JW, Greinert J, Herguera JC, Perez ME (2007) Authigenic carbon entombed in methane-soaked sediments from the northeastern transform margin of the Guaymas Basin, Gulf of California. Deep-Sea Res II-Topical Stud Oceanogr 54:1240–1267

Peckmann J, Thiel V (2004) Carbon cycling at ancient methane-seeps. Chem Geol 205:443–467

Peckmann J, Thiel V, Michaelis W, Clari P, Gaillard C, Martire L, Reitner J (1999) Cold seep deposits of Beauvoisin (Oxfordian; southeastern France) and Marmorito (Miocene; northern Italy): microbially induced authigenic carbonates. Int J Earth Sci 88:60–75

Quigley DC, Hornafius JS, Luyendyk BP, Francis RD, Clark J, Washburn L (1999) Decrease in natural marine hydrocarbon seepage near Coal Oil Point, California, associated with offshore oil production. Geology 27:1047–1050

Ramirez-Alvarez N, Macias-Zamora JV, Burke RA, Rodriguez-Villanueva LV (2007) Use of delta(13)C, delta(15)N, and carbon to nitrogen ratios to evaluate the impact of sewage-derived particulate organic matter on the benthic communities of the Southern California Bight. Environ Toxicol Chem 26:2332–2338

Reeburgh WS (2007) Oceanic methane biogeochemistry. Chem Rev 107:486–513

Reitner J, Peckmann J, Blumenberg M, Michaelis W, Reimer A, Thiel V (2005) Concretionary methane-seep carbonates and associated microbial communities in Black Sea sediments. Palaeogeogr Palaeoclimatol Palaeoecol 227:18–30

Sahling H, Rickert D, Lee RW, Linke P, Suess E (2002) Macrofaunal community structure and sulfide flux at gas hydrate deposits from the Cascadia convergent margin, NE Pacific. Mar Ecol Prog Ser 231:121–138

Sassen R, Roberts HH, Carney R, Milkov AV, DeFreitas DA, Lanoil B, Zhang CL (2004) Free hydrocarbon gas, gas hydrate, and authigenic minerals in chemosynthetic communities of the northern Gulf of Mexico continental slope: relation to microbial processes. Chem Geol 205:195–217

Schwartz H, Sample J, Weberling KD, Minisini D, Moore JC (2003) An ancient linked fluid migration system: cold-seep deposits and sandstone intrusions in the Panoche Hills, California, USA. In: Woodside JM, Garrison RE, Moore JC, Kvenvolden KA (eds) Contr 7th Int Conf Gas in Marine Sediments, 7–11 October 2002, Baku, Azerbaijan. Geo-Mar Letters SI 23(3/4):340–350. doi:10.1007/s00367-003-0142-1

Silverberg N, Martinez A, Aguiniga S, Carriquiry JD, Romero N, Shumilin E, Cota S (2004) Contrasts in sedimentation flux below the southern California Current in late 1996 and during the El Nino event of 1997–1998. Estuarine Coastal Shelf Sci 59:575–587

Stakes DS, Orange D, Paduan JB, Salamy KA, Maher N (1999) Cold-seeps and authigenic carbonate formation in Monterey Bay, California. Mar Geol 159:93–109

Suess E, Torres ME, Bohrmann G, Collier RW, Greinert J, Linke P, Rehder G, Trehu A, Wallmann K, Winckler G, Zuleger E (1999) Gas hydrate destabilization: enhanced dewatering, benthic material turnover and large methane plumes at the Cascadia convergent margin. Earth Planet Sci Lett 170:1–15

Tryon MD, Brown KM, Torres ME (2002) Fluid and chemical flux in and out of sediments hosting methane hydrate deposits on Hydrate Ridge, OR, II: hydrological processes. Earth Planet Sci Lett 201:541–557

Valentine DL, Reeburgh WS (2000) New perspectives on anaerobic methane oxidation. Environ Microbiol 2:477–484

Wardlaw GD, Arey JS, Reddy CM, Nelson RK, Ventura GT, Valentine DL (2008) Disentangling oil weathering at a marine seep using GCxGC: broad metabolic specificity accompanies subsurface petroleum biodegradation. Environ Sci Technol 42:7166–7173